archives
of thermodynamics
Vol. **32**(2011), No. 3, 103–116
DOI: 10.2478/v10173-011-0016-2

New technique of the local heat flux measurement in combustion chambers of steam boilers

JAN TALER[a*]
DAWID TALER[b]
TOMASZ SOBOTA[a]
PIOTR DZIERWA

a Cracow University of Technology, Chair of Thermal Power Engineering al. Jana Pawła II 37, 31-864 Kraków, Poland

b Cracow University of Technology, Institute of Heat Engineering and Air Protection , ul. Warszawska 24, 31-155 Kraków, Poland

Abstract A new method for measurement of local heat flux to water-walls of steam boilers was developed. A flux meter tube was made from an eccentric tube of short length to which two longitudinal fins were attached. These two fins prevent the boiler setting from heating by a thermal radiation from the combustion chamber. The fins are not welded to the adjacent water-wall tubes, so that the temperature distribution in the heat flux meter is not influenced by neighbouring water-wall tubes. The thickness of the heat flux tube wall is larger on the fireside to obtain a greater distance between the thermocouples located inside the wall which increases the accuracy of heat flux determination. Based on the temperature measurements at selected points inside the heat flux meter, the heat flux absorbed by the water-wall, heat transfer coefficient on the inner tube surface and temperature of the water-steam mixture was determined.

Keywords: Heat flux measurement; Inverse heat conduction problem; Steam boiler; Slagging of combustion chambers; CFD simulation

*Corresponding author. E-mail address: taler@mech.pk.edu.pl

Nomenclature

f_i	–	measured flux-tube temperature, °C or K
h_{in}	–	heat transfer coefficient on the inner surface of the tube, W/(m^2 K)
$\mathbf{I}_n$	–	identity matrix
$\mathbf{J}$	–	Jakobian matrix of $\mathbf{T}$
k	–	thermal conductivity, W/(m K)
m	–	number of measuring points
n	–	number of unknown parameters
q_m	–	absorbed heat flux, W/m^2
r_{in}	–	inner radius of the flux-tube, m
$\mathbf{r}$	–	position vector
s	–	extended coordinate along the fireside water-wall surface, mm
S	–	sum of the least squares
T_f	–	fluid temperature, °C or K
T_i	–	calculated temperature at the location r_i, °C or K
$\mathbf{T}^m$	–	m-dimensional column vector of calculated temperatures
x_i	–	unknown parameter
$\mathbf{x}$	–	n-dimensional column vector of unknown parameters

Greek symbols

μ	–	multiplier in the Levenberg-Marquardt algorithm
ψ	–	view factor

1 Introduction

Measurements of heat flux and heat transfer coefficient are subject of many current studies [1–4]. A proper understanding of combustion and heat transfer in furnaces and heat exchange on the water-steam side in water-walls requires accurate measurement of heat flux which is absorbed by membrane furnace walls [5–13]. There are three broad categories of heat flux measurements of the boiler water-walls: (1) portable heat flux meters inserted in inspection ports [3-4], (2) Gardon type heat flux meters welded to the sections of the boiler tubes [3–7], (3) tubular type instruments placed between two adjacent boiler tubes [8–13]. Tubular type and Gardon meters strategically placed on the furnace tube wall can be a valuable boiler diagnostic device for monitoring of slag deposition [14–16] If a heat flux instrument is to measure the absorbed heat flux correctly, it must resemble the boiler tube as closely as possible so far as radiant heat exchange with the flame and surrounding surfaces is concerned. Two main factors in this respect are emissivity and temperature of the absorbing surface, but since the instrument will almost always be coated with ash, it is generally the properties of the ash and not of the instrument that dominate the problem. Unfortunately, the thermal conductivity of the boiler tube can vary significently. Therefore, accurate measurements will only be performed if the deposit on the meter is representative of that on the surrounding tubes. The tubular type instruments known also as flux-tubes meet this requirement. In these devices the measured boiler tube wall temperatures are used for the evaluation of heat flux.

The measuring tube is fitted with two thermocouples in holes of known radial spacing r_1 and r_2. The thermocouples are led away to the junction box where they are connected differentially to give a flux related electromotive force.

The use of the one dimensional heat conduction equation for determining temperature distribution in the tube wall leads to the simple formula

$$q_m = \frac{k\,(f_1 - f_2)}{r_o \ln{(r_1/r_2)}} \;, \tag{1}$$

where f_1 and f_2 are measured wall temperatures at the locations r_1 and r_2, respectively and r_o is the outer radius of the tube. The accuracy of this equation is very low because of the circumferential heat conduction in the tube wall.

However, the measurement of heat flux absorbed by water-walls with satisfactory accuracy is a challenging task. Considerable work has been done in recent years in this field [8–13]. Previous attempts to accurately measure the local heat flux to membrane water-walls in steam boilers failed due to calculation of inside heat transfer coefficients. The heat flux can be only determined accurately if the inside heat transfer coefficient will be measured experimentally [8–9,12–13].

In this study, a numerical method for determining the heat flux in boiler furnaces, based on experimentally acquired interior flux-tube temperatures, is presented. The tubular type instrument has been designed (Fig. 1) to provide a very accurate measurement of absorbed heat flux q_m, inside heat transfer coefficient h_{in}, and water-steam temperature T_f. The number of thermocouples is greater than three because the additional information can help to enhance the accuracy of parameter determination. In contracts to the existing devices, in the developed flux-tube fins are not welded to adjacent water-wall tubes. Temperature distribution in the flux-tube is symmetric and not disturbed by different temperature fields in neighboring tubes.

The temperature dependent thermal conductivity of the flux-tube material was assumed. The meter is constructed from a short length of eccentric tube containing four thermocouples on the fireside below the inner and outer surfaces of the tube. The fifth thermocouple is located at the rear of the tube (on the casing side of the water-wall tube). The boundary conditions on the outer and inner surfaces of the water flux-tube must then be determined from temperature measurements in the interior locations. Four K-type sheathed thermocouples, 1 mm in diameter, are inserted into holes, which are parallel to the tube axis. The thermal conduction effect at the hot junction is minimized because the thermocouples pass through isothermal holes. The thermocouples are brought to the rear of the tube in the slot machined in the tube wall. An austenitic cover plate with thickness of 3 mm – welded to the tube – is used to protect the thermocouples from the incident flame radiation. A K-type sheathed thermocouple with a pad is used to measure the temperature at the rear of the flux-tube. This temperature is almost the same as the water-steam temperature.

The inverse problem of heat conduction was solved using the least squares method. Three unknown parameters were estimated using the Levenberg-Marquardt method. At every iteration step, the temperature distribution over the cross-section of the heat flux meter was computed using the ANSYS CFX software. Test calculations were carried out to assess accuracy of the presented method. The uncertainty in determined parameters was calculated using the Gauss variance propagation rule. The presented method is appropriate for membrane water-walls (Fig. 1). The new method has advantages in terms of simplicity and flexibility.

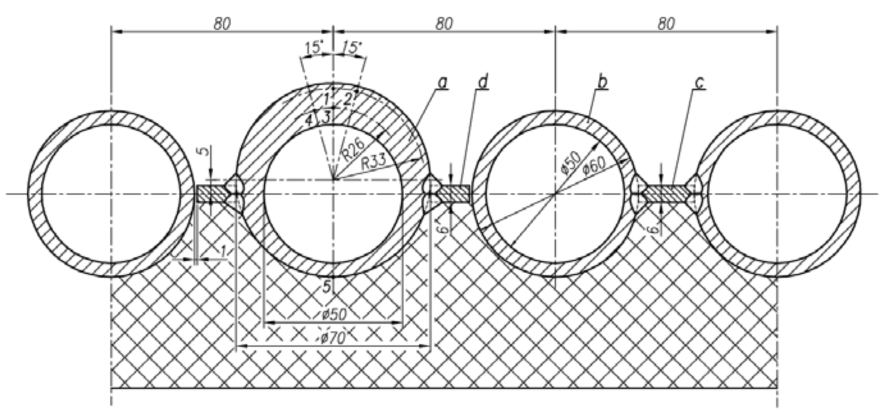

Figure 1. The cross-section of the membrane wall in the combustion chamber of the steam boiler.

2 Theory

The furnace wall tubes in most modern units are welded together with steel bars (fins) to provide membrane wall panels which are insulated on one side and exposed to a furnace on the other, as shown schematically in Fig. 1. The flux-tubes (Fig. 2) were manufactured in the laboratory and then securely welded to the water-wall tubes at different elevations in the furnace of the steam boiler. The coal fired boiler produces 58.3 kg/s superheated steam at 11 MPa and 540 °C.

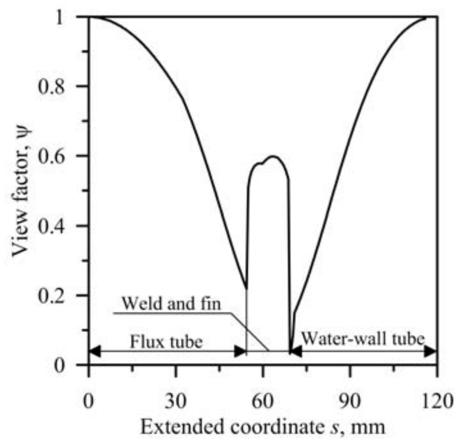

Figure 2. View factor distribution on the outer surface of water-wall tube.

Because of the symmetry, only the representative water-wall section illustrated in Fig. 3 needs to be analysed. In a heat conduction model of the flux-tube the following assumptions are made:

- temperature distribution is two-dimensional and steady-state,
- the thermal conductivity of the flux-tube and membrane wall may be dependent of temperature,
- the heat transfer coefficient h_{in} and the scale thickness ds is uniform over the inner tube surface.

The temperature distribution is governed by the non-linear partial differential equation [13]

$$\nabla \cdot [k(T)\nabla T] = 0 , \tag{2}$$

where ∇ is the vector operator, which is called nabla, and in Cartesian coordinates is defined by $\nabla = \mathbf{i}\partial/\partial x + \mathbf{j}\partial/\partial y + \mathbf{k}\partial/\partial z$. The unknown

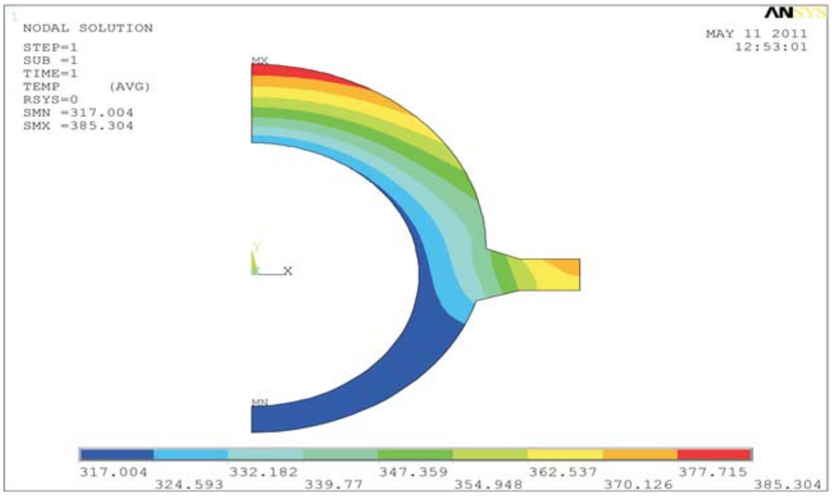

Figure 3. Temperature distribution in the flux tube cross-section for: q_m = 150000 W/m^2, T_f = 317 °C and h_{in} = 27000 W/(m^{2}K).

boundary conditions may be expressed as

$$\left[k\left(T\right)\frac{\partial T}{\partial n}\right]\bigg|_s = q\left(s\right) \ , \tag{3}$$

where $q(s)$ is the radiation heat flux absorbed by the exposed flux-tube and membrane wall surface. The local heat flux $q(s)$ is a function of the view factor $\psi(s)$ (Fig. 4)

$$q\left(s\right) = q_m\psi\left(s\right) \ , \tag{4}$$

where q_m is measured heat flux (thermal loading of heating surface). The view factor $\psi(s)$ from the infinite flame plane to the differential element on the membrane wall surface can be determined graphically, Taler [16], or numerically. In this paper, $\psi(s)$ was evaluated numerically using the finite element program ANSYS [17], and is displayed in Fig. 4 as a function of extended coordinate s.

The convective heat transfer from the inside tube surfaces to the water-steam mixture is described by the Newton's law of cooling

$$-\left[k\left(T\right)\frac{\partial T}{\partial n}\right]\bigg|_{s_{in}} = h_{in}\left(T|_{s_{in}} - T_f\right) \ , \tag{5}$$

where $\partial T/\partial n$ is the derivative in the normal direction, h_{in} is the heat transfer coefficient and T_f denotes the temperature of the water-steam mixture.

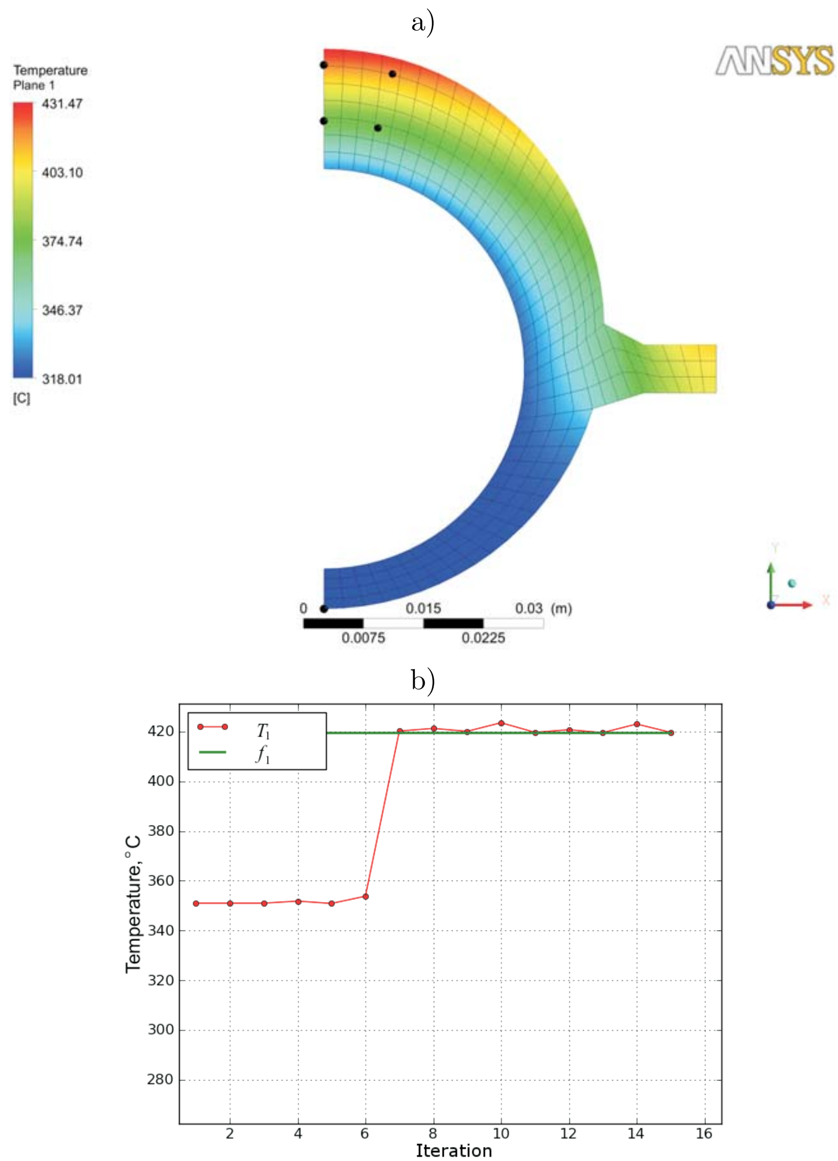

Figure 4. Temperature distribution (a) in the flux-tube obtained from the solution of the inverse problem for the "exact" data: f_1 = 419.66 °C, f_2 = 417.31 °C, f_3 = 374.90 °C, f_4 = 373.19 °C, f_5 = 318.01 °C and iteration number (b) for the temperature T_1.

The reverse side of the membrane water-wall is thermally insulated.

In addition to the unknown boundary conditions, the internal temperature measurements f_i are included in the analysis

$$T_e(\mathbf{r}_i) = f_i, \quad i = 1, \ldots, m \;, \tag{6}$$

where $m = 5$ denotes the number of thermocouples (Fig. 3). The unknown parameters: $x_1 = q_m$, $x_2 = h_{in}$, and $x_3 = T_f$ were determined using the least-squares method. The symbol r_{in} denotes the inside tube radius, and $k(T)$ is the temperature dependent thermal conductivity. The object is to choose $\mathbf{x} = (x_1, \ldots, x_n)^T$ for $n = 3$ such that computed temperatures $T(\mathbf{x}\ \mathbf{r}_i)$ agree within certain limits with the experimentally measured temperatures f_i.

This may be expressed as

$$T(\mathbf{x}, \mathbf{r}_i) - y_i \cong 0, \quad i = 1, \ldots, m, \quad m = 5 \;. \tag{7}$$

The least-squares method is used to determine parameters $\mathbf{x}$. The sum of squares

$$S = \sum_{i=1}^{m} [f_i - T(\mathbf{x}, \mathbf{r}_i)]^2, \quad m = 5 \tag{8}$$

can be minimized by a general unconstrained method.

However, the properties of (8) make it worthwhile to use methods designed specifically for the nonlinear least-squares problem. In this paper, the Levenberg–Marquardt method [18,19] is used to determine the parameters x_1, x_2 and x_3. The Levenberg–Marquardt method performs the k-th iteration as

$$\mathbf{x}^{(k+1)} = \mathbf{x}^{(k)} + \delta^{(k)} \;, \tag{9}$$

where

$$\delta^{(k)} = \left[\left(\mathbf{J}^{(k)}\right)^T \mathbf{J}^{(k)} + \mu \mathbf{I_n} \right]^{-1} \left(\mathbf{J}^{(k)}\right)^T \left[\mathbf{f} - \mathbf{T}\left(\mathbf{x}^{(k)}\right) \right], \quad k = 0, 1, \ldots, \tag{10}$$

where μ is the multiplier and $\mathbf{I}_n$ is the identity matrix. The Levenberg–Marquardt method is a combination of the Gauss–Newton method ($\mu^{(k)} \to 0$) and the steepest-descent method ($\mu^{(k)} \to \infty$) The m x n of $T(\mathbf{x}^{(k)}, \mathbf{r}_i)$ is given by

$$\mathbf{J}^{(k)} = \left.\frac{\partial \mathbf{T}\left(\mathbf{x}\right)}{\partial \mathbf{x}_T}\right|_{\mathbf{x}=\mathbf{x}^{(k)}} = \left.\begin{bmatrix} \frac{\partial T_1}{\partial x_1} & \cdots & \frac{\partial T_1}{\partial x_n} \\ \cdots & \cdots & \cdots \\ \cdots & \cdots & \cdots \\ \cdots & \cdots & \cdots \\ \cdots & \cdots & \cdots \\ \frac{\partial T_m}{\partial x_1} & \cdots & \frac{\partial T_m}{\partial x_n} \end{bmatrix}\right|_{\mathbf{x}=\mathbf{x}^{(k)}} , \quad m = 5, \quad n = 3 , \tag{11}$$

where $\mathbf{T}(\mathbf{x}^{(k)}) = (T_1^{(k)}, \ \ldots \ T_m^{(k)})^T$. The iterative procedure is continued until the changes in $x_i^{(k)}$, $i = 1, \ldots n$ are less than some small amount ε.

At every k-th iteration step the temperature distribution $\mathbf{T}(\mathbf{x}^{(k)}, \mathbf{r}_i)$ is calculated. The boundary value problem given by Eq. (2) and boundary conditions (3) and (5) was solved at each iteration step by the finite element method (FEM). The uncertainties of the determined parameters $\mathbf{x}$ may be estimated using the error propagation rule of Gauss, suggested by Press *et al.* [20].

3 Uncertainty analysis

The uncertainties of the determined parameters $\mathbf{x}^*$ will be estimated using the error propagation rule of Gauss [16,18]. The propagation of uncertainty in the independent variables: measured wall temperatures f_j, $j = 1, \ldots \ m$ and thermal conductivity k is estimated from the following equation:

$$2\sigma_{x_i} = \left[\sum_{j=1}^{m}\left(\frac{\partial x_i}{\partial f_j}2\sigma_{f_j}\right)^2 + \left(\frac{\partial x_i}{\partial k}2\sigma_k\right)^2\right]^{\frac{1}{2}} , \quad i = 1, 2, 3 \, . \tag{12}$$

The 95% uncertainty in the estimated parameters can be expressed in the form

$$x_i = x_i^* \pm 2\sigma_{x_i} \; ,$$

where $x_i = x_i^* \quad i = 1 \ 2 \ 3$ represent the value of the parameters obtained using the least squares method. The sensitivity coefficients $\partial x_i / \partial f_j$ and $\partial x_i / \partial k$ in Eq. (12) were calculated by means of the numerical approximation using central difference quotients.

4 Test computations

The material of the heat flux-tube is 20G steel. The composition of the 20G mild steel is as follows: 0.17–0.24% C, 0.7–1.0% Mn, 0.15–0.40% Si, Max 0.04% P, Max 0.04% S, and the remainder is iron Fe. The heat flux-tube thermal conductivity is assumed to be temperature dependent (Tab. 1).

Table 1. Thermal conductivity $k(T)$ of steel 20G as a function of temperature.

Temperature, °C	100	200	300	400
Thermal conductivity, W/(m K)	50.69	48.60	46.09	42.30

To demonstrate that the maximum temperature of the fin tip is lower than the allowable temperature for the 20G steel, the flux-tube temperature was computed using ANSYS CFX package [17]. Changes of the view factor on the flux tube, weld and fin surface were calculated with ANSYS CFX. The temperature distribution shown in Fig. 3 was obtained for the following data: absorbed heat flux, $q_m = 150000$ W/m^2, temperature of the water-steam mixture, $T_f = 317$ °C, and heat transfer coefficient at the tube inner surface, $h_{in} = 27000$ W/(m^{2}K). An inspection of the results shown in Fig. 3 indicates that the maximum temperature of the fin does not exceed 375 °C. Next, to illustrate the effectiveness of the presented method, test calculations were carried out. The thermal conductivity of the 20G steel was approximated by the function

$$k(T) = 53.26 - 0.02376224T,$$

where k is expressed in W/(m K) and temperature T in °C.

The "measured" temperatures f_i, $i = 1, 2, \ldots, 5$ were generated artificially by means of ANSYS CFX for: $q_m = 250000$ W/m^2, $h_{in} = 30000$ W/(m^{2}K) and $T_f = 318$ °C. The following values of "measured" temperatures were obtained $f_1 = 419.66$ °C, $f_2 = 417.31$ °C, $f_3 = 374.90$ °C, $f_4 = 373.19$ °C, $f_5 = 318.01$ °C. The temperature distribution in the flux tube cross-section, reconstructed on the basis of five measured temperatures is depicted in Figure 4a. The proposed inverse method is very accurate since the estimated parameters: $q_m = 250000.063$ W/m^2, $h_{in} = 30000.054$ W/(m^{2}K) and $T_f = 318.0$ °C differ insignificantly from the input values. In order to show the influence of measurement errors on the determined parameters, the 95% confidence intervals were estimated. The following uncertainties of the measured values were assumed (at 95% confidence interval): $2\sigma_{f_j} = \pm 0.5K$, $j = 1, 2, \ldots, 5$, $2\sigma_k = \pm 1$ W(m K). The uncertainties (95% confidence interval) of the coefficients x_i were determined using the error propagation rule formulated by Gauss [18–20] The calculated uncertainties are: ±6% for q_m, ±33% for h_{in} and ±0.3% for T_f. The accuracy of the results obtained is acceptable.

Then, the inverse analysis was carried out for perturbed data: $f_1 =$ 420.16 °C, $f_2 = 416.81$ °C, $f_3 = 375.40$ °C, $f_4 = 372.69$ °C, $f_5 = 318.01$ °C. The reconstructed temperature distribution illustrates Fig. 5b. The obtained results are: $q_m = 250118.613$ W/m^2, $h_{in} = 30050.041$ W/(m^2 K) and $T_f = 317.99$ °C. The influence of the error in the measured temperatures on the estimated parameters is small.

The number of iterations in the Levengerg-Marquardt procedure is small in both cases (Figs. 4b and 5b).

5 Conclusions

A CFD based method for determining heat flux absorbed water-wall tubes, heat transfer coefficient at the inner flux tube surface and temperature of the water-steam mixture has been presented. A new flux tube type was proposed. Fins attached to the flux tube are not welded to the adjacent water-wall tubes, so the temperature distribution in the measuring device is not affected by neighboring water-wall tubes. The installation of the flux tube is easier because welding of fins to adjacent water-wall tubes is avoided. Based on the measured flux tube temperatures the non-linear inverse heat conduction problem was solved. The number of thermocouples placed inside the heat flux-tube including the thermocouple on the rear outer tube surface is greater than the number of unknown parameters because additional measurement points reduces the uncertainty in determined parameters. The proposed flux tube and the inverse procedure for determining absorbed heat flux can be used both when the inner surface of the heat flux tube is clean and when scale or corrosion deposits are presents on the inner surface what can occur after a long time service of the heat flux-tube. The flux tube can work for a long time in the destructive high temperature atmosphere of a coal-fired boiler.

Received 10 October 2011

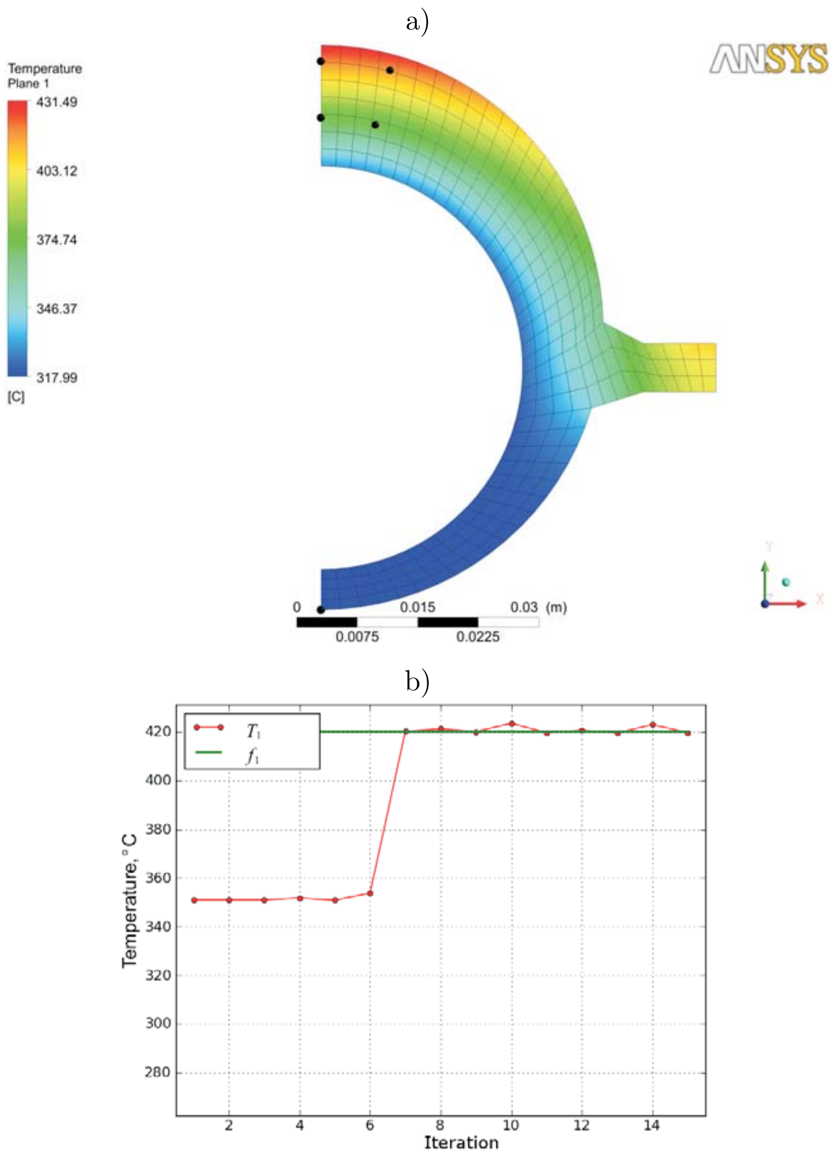

Figure 5. Temperature distribution (a) in the flux-tube obtained from the solution of the inverse problem for the "perturbed" data: f_1 = 420.16 °C, f_2 = 416.81 °C, f_3 = 375.40 °C, f_4 = 372.69 °C, f_5 = 318.01 °C and iteration number (b) for the temperature T_1.

References

[1] Taler D., Grądziel S., Taler J.: *Measurement of heat flux density and heat transfer coefficient*. Archives of Thermodynammics, **31**(2010), 3–18.

[2] Sobota T.: *Experimental prediction of heat transfer correlations in heat exchangers*. Chapter in: Developments in heat transfer (M.A.S Bernardes, ed.), In-Tech, Vienna – Rijeka 2011, ISBN 978-953-307-569-3.

[3] Taler J., Taler D.: *Measurement of heat flux and heat transfer coefficient*. Chapter in: Heat Flux: Processes, Measurement Techniques and Applications (G. Cirimele, M. D'Elia eds.), Nova Science Publishers, Inc., New York 2011, ISBN: 978-1-61470-887-2.

[4] Seeger M., Taler J.: *Konstruktion und Einsatz transportabler Warmeflussonden zur Bestimmung der Heizflachenbelastung in Feuerraumen*. Fortschr.-Ber. VDI Zeitschrift Reihe 6, 129 VDI-Verlag Dusseldorf 1983.

[5] Northover E. W., Hitchcock J. A.: *A heat flux meter for use in boiler furnaces*. J Sci. Instrum **44**(1967), 371–374.

[6] Neal S. B. H. C., Northover E. W.: *The measurement of radiant heat flux in large boiler furnaces-I. Problems of ash deposition relating to heat flux*. Int J Heat Mass Transfer **23**(1980), 1015–1022.

[7] Arai N., Matsunami A., Churchill S. W.: *A review of measurements of heat flux density applicable to the field of combustion*. Exp Therm Fluid Sci. **12**(1996), 452–460.

[8] Taler J.: *Measurement of heat flux to steam boiler membrane water walls*. VGB Kraftwerkstechnik **70**(1990), 540–546.

[9] Taler J.: *A method of determining local heat flux in boiler furnaces*. Int. J Heat Mass Transfer **35**(1992), 1625–1634.

[10] Fang Z., Xie D., Diao N., Grace J. R., Jim Lim C.: *A new method for solving the inverse conduction problem in steady heat flux measurement*. Int J Heat Mass Transfer **40**(1997), 3947–3953.

[11] Luan W., Bowen B. D., Lim C. J., Brereton C. M. H., Grace J. R.: *Suspension-to membranewall heat transfer in a circulating fluidized bed combustor*. Int J. Heat Mass Transfer **43**(2000), 1173–1185.

[12] Sobota T., Taler D.: *The measurement of radiant heat flux in combustion chambers of large steam boilers*. In: Proc. 8th World Congress on Computational Mechanics (WCCM8), 5th European Congress on Computational Methods in Applied Sciences and Engineering (ECCOMAS 2008), Venice, June 30 – July 4, 2008.

[13] Sobota T., Taler D.: *A simple method for measuring heat flux in boiler furnaces*, Rynek Energii **86**(2010), 108-114.

[14] Valero A., Cortes C.: *Ash fouling in coal-fired utility boilers. Monitoring and optimization of on-load cleaning*. Prog Energy Combust Sci **22**(1996), 189–200.

[15] Teruel E., Cortes C., Diez L. I., Arauzo I.: *Monitoring and prediction of fouling in coal-fired utility boilers using neural networks*. Chem Eng Sci. **60**(2005), 5035–5048.

[16] Taler J., Trojan M., Taler D.: *Monitoring of ash fouling and internal scale deposits in pulverized coal fired boilers*. Chapter in: Advances in mechanical engineering research, Vol. 1, (D.E. Malach ed.). Nova Science Publishers, Inc., New York 2011, ISBN 978-1-61761-110-0.

[17] ANSYS CFX 12. ANSYS Inc., Urbana, Illinois, USA, 2010.

[18] Seber G.A.F., Wild C.J.: *Nonlinear Regression*. Wiley New York 1989.

[19] it Policy on reporting uncertainties in experimental measurements and results. Trans. ASME J Heat Transfer **122**(2000), 411–413.

[20] Press W.H. *et al*: *Numerical Recipes in Fortran. The Art Of Scientific Computing*. Cambridge University Press CambridgeLondon 1992.